

# Electromagnetic form factors in the time like region with PANDA

---

María Carmen Mora Espí

Institut für Kernphysik, Johannes Gutenberg Universität, Mainz  
GSI, Darmstadt

---

Institutsseminar  
12. Januar 2009



# Outline

- 1 **Introduction**
  - Electromagnetic Form Factors in the time like region
  - Measurement of the electromagnetic Form Factors
  - Available data
- 2  **$\bar{P}$ ANDA detector**
- 3 **Simulations and analysis**
  - Description of the analysis
  - Electron analysis
  - Muon analysis
- 4 **Conclusions and Outlook**



## Electromagnetic Form Factors

Parameterize the hadronic current in the matrix element for elastic electron scattering and its crossed process annihilation.

### Matrix element for e-p scattering:

$$M = \frac{e^2}{q^2} \bar{u}(k_2) \gamma^\mu u(k_1) \bar{u}(p_2) \left[ F_1(q^2) \gamma_\mu + i \frac{\sigma_{\mu\nu} q^\nu}{2M} F_2(q^2) \right] u(p_1)$$

$F_1$ : Dirac FF  
 $F_2$ : Pauli FF

One can define the **Sachs Form Factors** as:

$$G_e = F_1 + \tau F_2$$

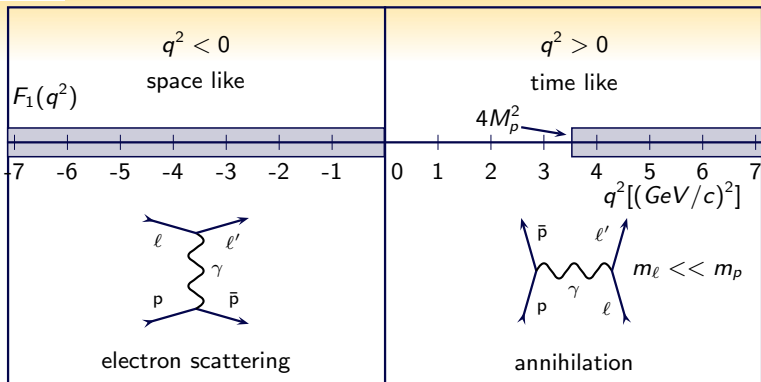
$$G_m = F_1 + F_2$$

$$\text{where } \tau = \frac{q^2}{4M^2 c^4}$$

- Depend on transferred momentum,  $q^2$ .
- We are interested in measuring the Electromagnetic Form Factors in **time-like** region.



## Space-like and Time-like regions



- |                                                                      |                                                               |
|----------------------------------------------------------------------|---------------------------------------------------------------|
| • No threshold                                                       | • Threshold at $q^2 = 4M_p^2$                                 |
| • Real functions                                                     | • Complex functions                                           |
| • Fourier transform of spatial charge and magnetization distribution | • Fourier transform of the response of nucleon in time domain |
| • Well known                                                         | • Not well known                                              |

Space-like and Time-like regions are connected by **DISPERSION RELATIONS**.



## Access to time-like form factors

We can access via the reactions  $\bar{p}p \rightarrow \ell^+ \ell^-$

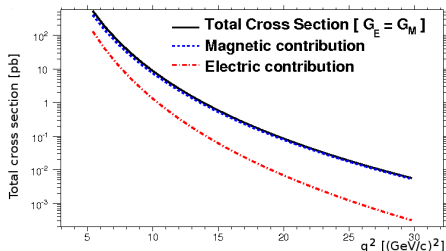
### Cross Section $\bar{p}p \rightarrow \ell^+ \ell^-$

$$\frac{d\sigma}{d\cos\theta} = \frac{\pi\alpha^2(\hbar c)^2}{8M_p\sqrt{\tau(\tau-1)}} \left[ |G_m|^2 (1 + \cos^2\theta) + \frac{|G_e|^2}{\tau} (1 - \cos^2\theta) \right]$$

- With **high statistics** one can measure the **angular distribution**.
- Knowing the luminosity one can calculate the **differential cross section**.

$$\frac{d\sigma}{d\cos\theta} = \frac{1}{L} \frac{d^2N}{dt \cdot d\cos\theta}$$

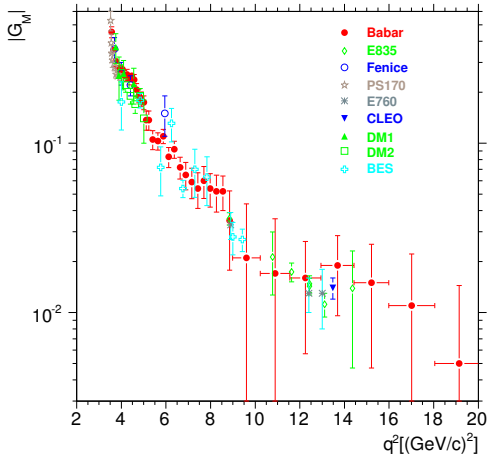
- The **total cross section** can be calculated from the total **number of signal events**.





# World data on time-like electromagnetic Form Factors

Available data so far had low statistics except BABAR and PS170 experiments.

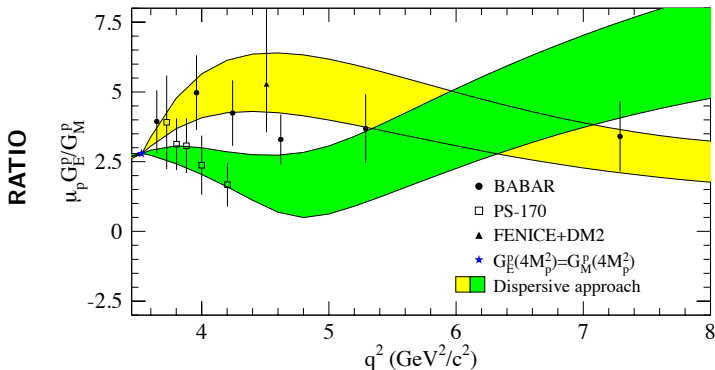


- Assumption of equality between  $G_e$  and  $G_m$  (Valid strictly only at threshold).

- BABAR: 3284 events
- E835: 206 events
- Fenice: 25 and 69 events
- PS170: 3667 events
- E760: 29 events
- CLEO: 14 events
- DM1: 63 events
- DM2: 172 events
- BES: 90 events



## Fit to Form Factors data using dispersion relations



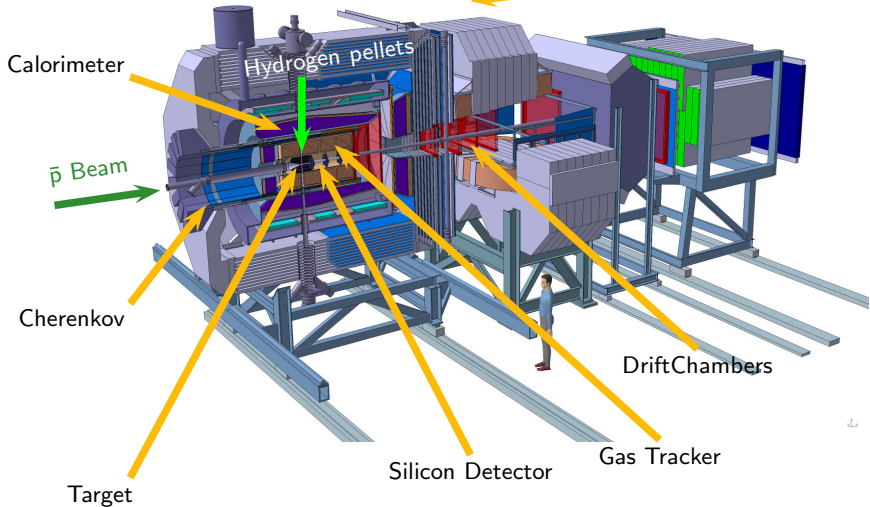
- A fit to the data (using also results in space-like region) show the possibility of  $G_E/G_M$  being 0, 1 or even 3
- Discrepancies between BABAR and PS-170 experiments.



# PANDA detector setup

Target Spectrometer

Forward Spectrometer







# PANDA challenges and capabilities

- 1.- Nucleon structure studies: Measurement of FF in time-like region.
- 2.- Physics case:

- Study of reaction by the signal channels  $\bar{p}p \rightarrow e^+e^-$  and  $\bar{p}p \rightarrow \mu^+\mu^-$ .
- Background channels:

- $\bar{p}p \rightarrow \pi^+\pi^- \rightarrow 10^6$  times higher than signal in average.
- $\bar{p}p \rightarrow \pi^0\pi^0$
- $\bar{p}p \rightarrow \pi^0\gamma$
- $\bar{p}p \rightarrow \gamma\gamma$

- **Challenge:** Good suppression of pions as background.

- 3.- Panda Detector:

- High Luminosity:  $L = 2 \cdot 10^{32} \text{ cm}^{-2}\text{s}^{-1}$
- Good tracking system.
- Good PID capabilities.

→ SIMULATION



## Simulation and analysis description

- 1.- EvtGen.
- 2.- GEANT4.
- 3.- Digitization.
- 4.- Cluster and track finding.
- 5.- Reconstruction.
  - Candidates selection: Reconstruction of **events**.
  - Particle Identification: Using different likelihood levels on different detectors → **PID** lists for different particle hypothesis ( $e$ ,  $\mu$ ,  $p$ ,  $\pi$  and  $K$ ):
    - Charged
    - Very loose
    - Loose
    - Tight
    - Very Tight

(Increasing likelihood level from top to bottom)
- 6.- **Kinematical fits** to reconstructed tracks.
- 7.- Final event selection **Fits** on particle candidate properties.
- 8.- Results: **Fit** to reconstructed **angular distribution**.



## Simulation and analysis description

- 1.- EvtGen.
- 2.- GEANT4.
- 3.- Digitization.
- 4.- Cluster and track finding.
- 5.- Reconstruction.
  - Candidates selection: Reconstruction of **events**.
  - Particle Identification: Using different **likelihood** levels on different detectors → **PID** lists for different particle hypothesis ( $e$ ,  $\mu$ ,  $p$ ,  $\pi$  and  $K$ ):
    - Charged
    - Very loose
    - Loose
    - Tight
    - Very Tight

(Increasing likelihood level from top to bottom)
- 6.- **Kinematical fits** to reconstructed tracks.
- 7.- Final event selection **cuts** on particle candidate properties.
- 8.- Results: **Fit** to reconstructed **angular distribution**.

# ANALYSIS



## Simulation and analysis description

- 1.- EvtGen.
- 2.- GEANT4.
- 3.- Digitization.
- 4.- Cluster and track finding.
- 5.- Reconstruction.
  - Candidates selection: Reconstruction of **events**.
  - Particle Identification: Using different **likelihood** levels on different detectors → **PID** lists for different particle hypothesis ( $e$ ,  $\mu$ ,  $p$ ,  $\pi$  and  $K$ ):
    - Charged
    - Very loose
    - Loose
    - Tight
    - Very Tight

(Increasing likelihood level from top to bottom)
- 6.- **Kinematical fits** to reconstructed tracks.
- 7.- Final event selection: **Cuts** on particle candidate properties.
- 8.- Results: **Fit** to reconstructed **angular distribution**.

# ELECTRON ANALYSIS



# Simulated events for analysis using electrons

Signal:

$p \text{ (GeV/c)}$	1.7	2.9	3.0	3.7	4.9	5.9	6.4	7.9	10.9
$q^2 \text{ [(GeV/c)}^2]$				8.2		12.9		16.7	
$e^+e^-$									
$G_e = 0$	$10^6$	$10^6$	$10^6$	$10^6$	$10^6$	$10^6$	$10^6$	$10^6$	$10^6$
$G_e = G_m$	$10^6$	$10^6$	$10^6$	$10^6$	$10^6$	$10^6$	$10^6$	$10^6$	$10^6$
$G_e = 3 \cdot G_m$	$10^6$	$10^6$	$10^6$	$10^6$	$10^6$	$10^6$	$10^6$	$10^6$	$10^6$

Background:

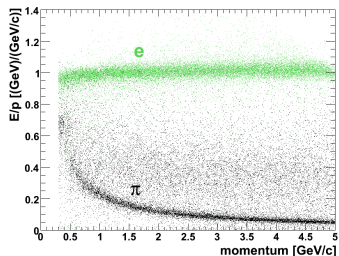
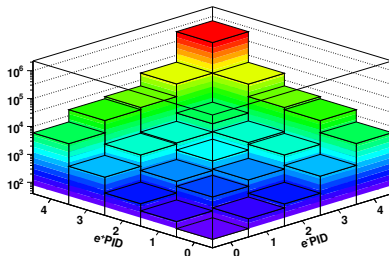
$p \text{ (GeV/c)}$	3.7	5.9	7.9
$q^2 \text{ [(GeV/c)}^2]$	8.2	12.9	16.7
$\pi^+\pi^-$	$10^8$	$10^8$	$2 \cdot 10^8$
$\pi^0\pi^0 \rightarrow$			
$\gamma\gamma + \gamma\gamma$	$10^6$	$10^6$	$10^6$
$\gamma\gamma + \gamma e^+e^-$	$10^6$	$10^6$	$10^6$
$\gamma e^+e^- + \gamma e^+e^-$	$10^6$	$10^6$	$10^6$

1 event - 2 s cpu time  $\rightarrow \approx 6$  cpu years in only 1 machine for 1 channel background simulation.



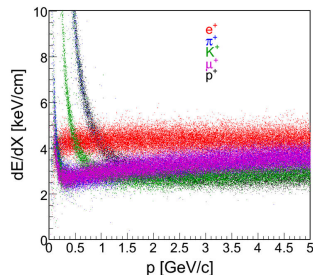
# Particle identification

epemGeGm3.3000GeVSP-359.root



## electron PID cuts:

- (0) Charged particles
- (1) Very Loose (VL) > 20%
- (2) Loose (L) > 85%
- (3) Tight (T) > 99%
- (4) Very Tight (VT) > 99.8% + 10%/detector





## Kinematical fit

- $E$  and  $p$  have been measured for each track.
- 4-constraints fit ( $E, p, m, r_0$ ) performed with some particle hypothesis ( $e, \mu, p, \pi$  and  $K$ ).
- Calculated the fit confidence level for each hypothesis.

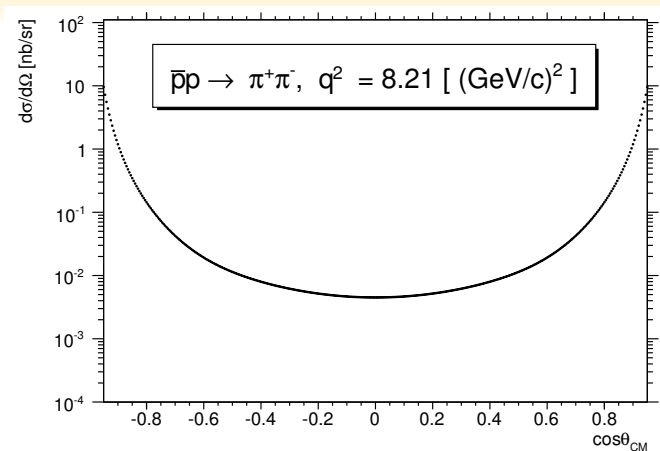
### Kinematical fit:

- $CL(e^+e^-) > 10 \cdot CL(\pi^+\pi^-)$
- $CL(e^+e^-) > 10^{-3} \rightarrow$  Necessary to suppress the whole  $\pi^0$  background.





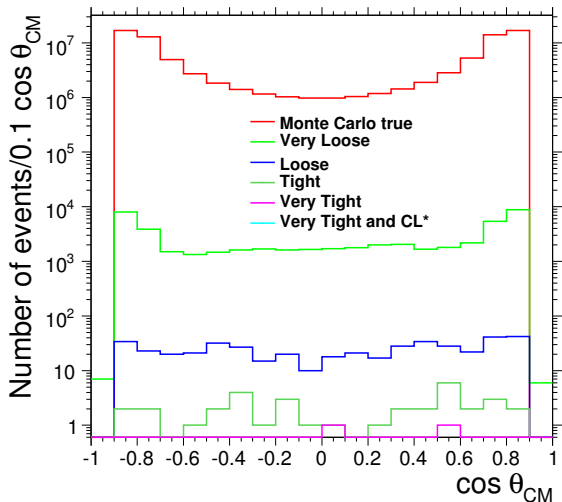
## $\bar{p}p \rightarrow \pi^+\pi^-$ cross section



- $\bar{p}p \rightarrow \pi^+\pi^-$  cross section is not well known.
- A model fitting the existing experimental data has been done as input for the simulation.



# Test of background suppression: $\bar{p}p \rightarrow \pi^+\pi^-$



$$p = 3.3 \text{ GeV}/c; q^2 = 8.2 (\text{GeV}/c)^2$$

Angular distribution of charged pions:

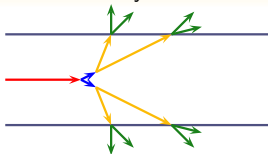
Background suppression with cuts:

- PID constraints:  
2 misidentified pions.
- CL and PID constraints:  
Background suppression of  $10^8$



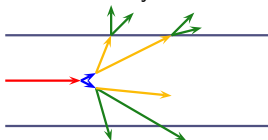
## Test of background suppression: $\bar{p}p \rightarrow \pi^0\pi^0$

Normal decay:



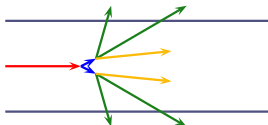
- protons
- pions
- photons
- electrons

1 Dalitz decay:



- Normal decay: Does not produce electrons near the vertex.
- 1 Dalitz decay: Produces 2 electrons near the vertex.
- 2 Dalitz decays: Produce 4 electrons near the vertex.

2 Dalitz decays

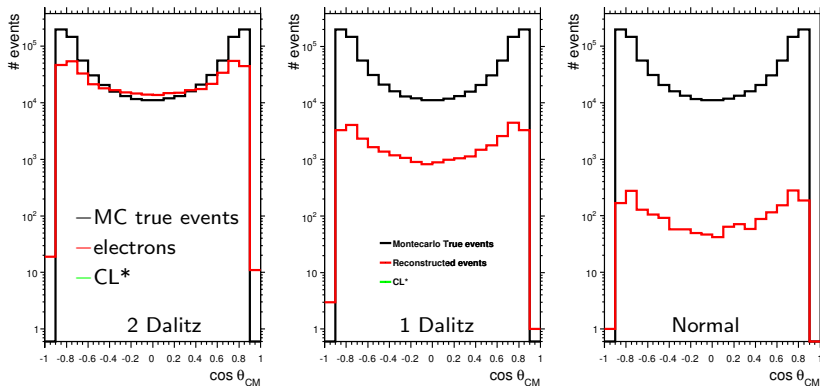


- Electrons from conversion of photons in the beam pipe are easily discriminated by kinematical constraints.
- Electrons from Dalitz decay can be confused with signal electrons.



# Test of background suppression: $\bar{p}p \rightarrow \pi^0\pi^0$

Angular distribution of neutral pions:  $p = 5.9 \text{ GeV}/c$ ;  $q^2 = 12.9 (\text{GeV}/c)^2$



- CL constraints suppress **all** background.
- PID constraints are **not** usefull.

Branching ratios:

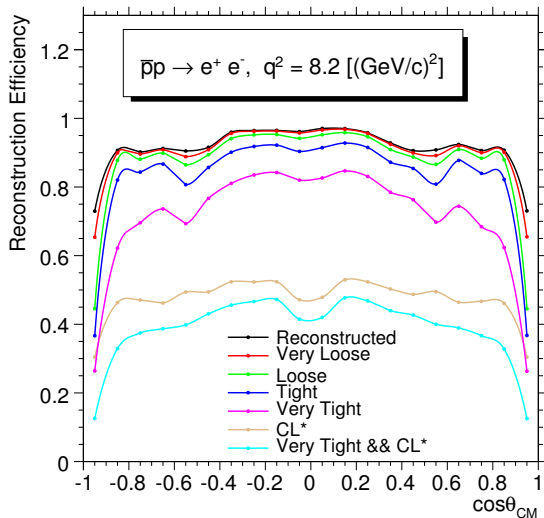
$$\Gamma_{2\gamma}/\Gamma_{tot} = 98.798\%$$

$$\Gamma_{e^+e^-\gamma}/\Gamma_{tot} = 1.198\%$$



## Signal: Reconstruction efficiency

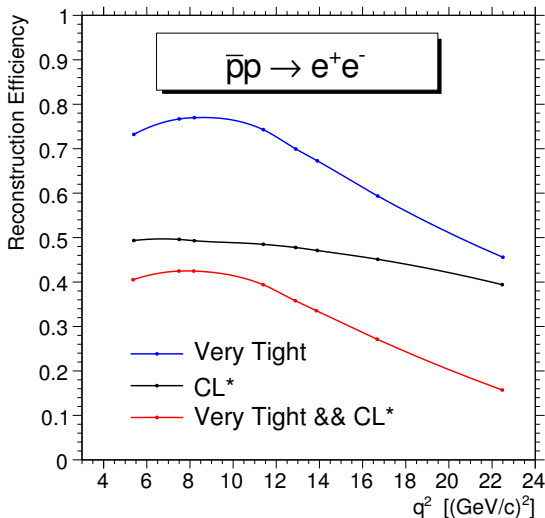
$$G_e = G_m; p = 3.3 \text{ GeV}/c; q^2 = 8.2 \text{ (GeV}/c)^2$$



- PID cuts don't represent a big suppression in efficiency.
- CL cut represents about 50% of signal reduction.
- After combination of PID and CL cuts the efficiency is about 40%.



## Signal: Reconstruction efficiency $G_e = G_m$ vs $q^2$



- At higher energies, the efficiency is smaller than at lower energies.
- In comparison with the expected statistics the angular distribution reconstruction is more difficult at higher energies.
- Results for  $G_e = 0$  and  $G_e = 3G_m$  are similar.



## Realistic statistics

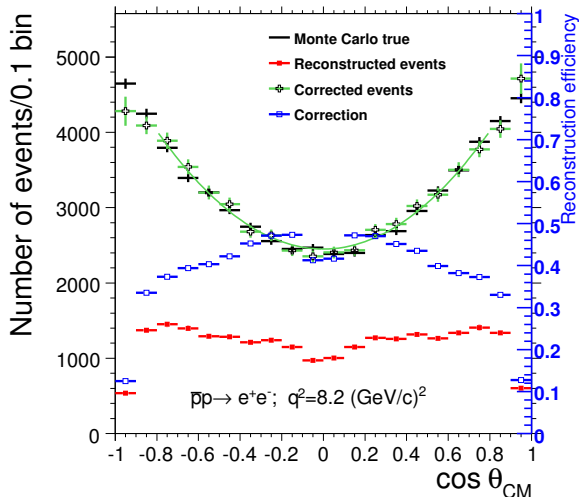
*Signal  $e^+e^-$ :*

At full luminosity ( $\mathcal{L} = 2 \cdot 10^{32} \text{ cm}^{-2}\text{s}^{-1}$ ) and  $10^7$  s of measurement time, corresponding approximately to 116 days, the expected number of events is the following:

$s(\text{GeV}/c)^2$	Nr. events
5.40	$1.07 \cdot 10^6$
7.43	$1.24 \cdot 10^5$
7.64	$1.03 \cdot 10^5$
8.20	$6.47 \cdot 10^4$
11.03	9078
12.90	3204
13.86	1985
16.69	572
22.29	81



## Signal: Angular distribution



$$G_e = 0;$$

$$p = 3.3 \text{ GeV/c};$$

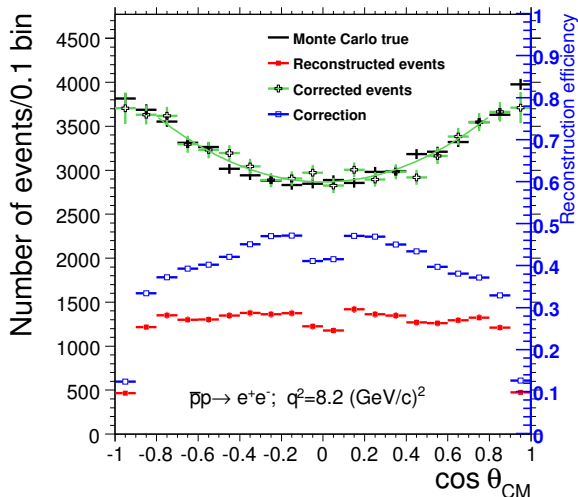
$$q^2 = 8.2 \text{ (GeV/c)}^2$$

- Realistic statistics: 64 000 events.
- Good angular distribution reconstruction after acceptance correction.
- The acceptance correction have been calculated using 1 000 000 events and isotropical distribution simulation.





## Signal: Angular distribution



$$G_e = G_m;$$

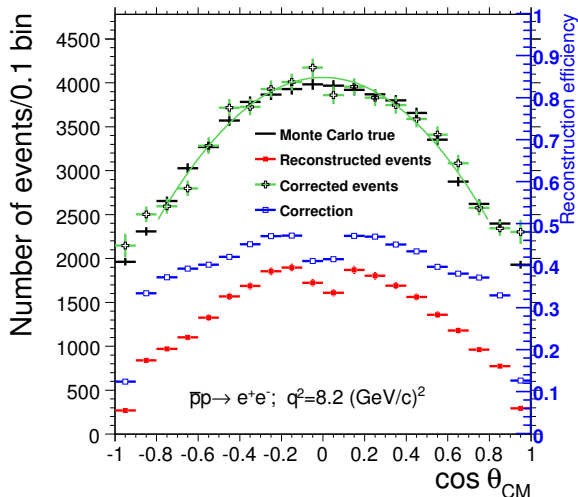
$$p = 3.3 \text{ GeV/c};$$

$$q^2 = 8.2 \text{ (GeV/c)}^2$$

- Realistic statistics: 64 000 events.
- Good angular distribution reconstruction after acceptance correction.
- The acceptance correction have been calculated using 1 000 000 events and isotropical distribution simulation.



## Signal: Angular distribution



$$G_e = 3G_m;$$

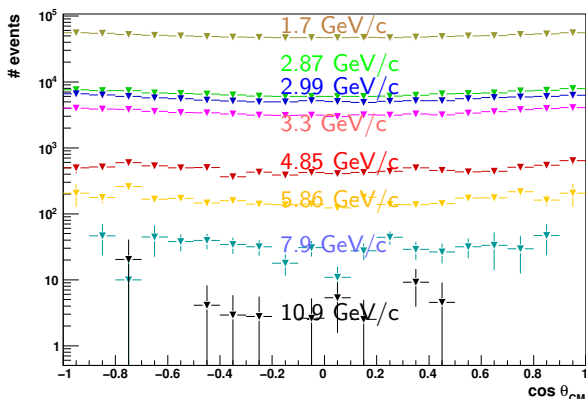
$$p = 3.3 \text{ GeV/c};$$

$$q^2 = 8.2 \text{ (GeV/c)}^2$$

- Realistic statistics: 64 000 events.
- Good angular distribution reconstruction after acceptance correction.
- The acceptance correction have been calculated using 1 000 000 events and isotropical distribution simulation.



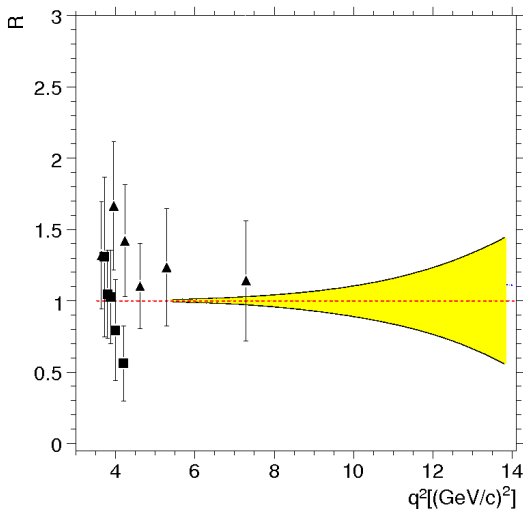
# Reconstructed and corrected angular distributions for $\bar{p}p \rightarrow e^+e^-$ and $G_e = G_m$ at different energies



- Angular distribution can be well reconstructed up to 5.8 GeV/c ( $12.9 \text{ (GeV/c)}^2$ ).
- At higher energies is still possible to use the integrated cross section for  $G_e/G_m$  calculation.



## Results for $G_e/G_m$



- Squares and triangles represent the values calculated in BABAR and PS170 experiments.
- Our results (for the case of  $G_e = G_m$ ) will be distributed around the red horizontal dashed line.
- The error bars of our calculations (only statistical) are represented by the yellow band.
- The errors are a factor 10 smaller than those calculated up to now.

# MUON ANALYSIS



# Simulated events for analysis using muons

Signal:

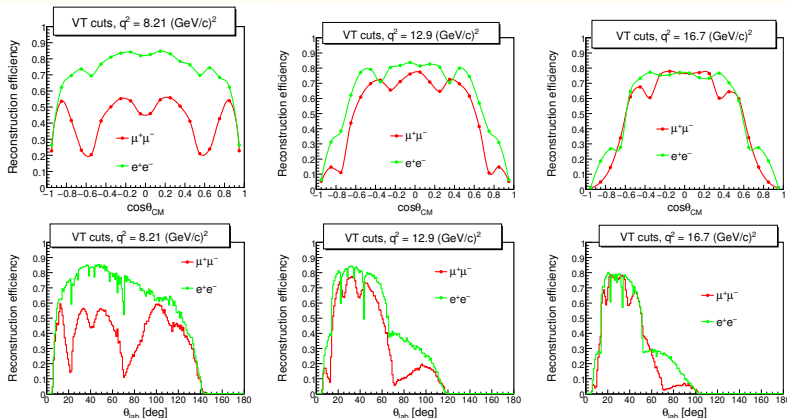
$p \text{ (GeV/c)}$	1.7	3.3	5.9	7.9
$q^2 \text{ [(GeV/c)}^2]$	5.4	8.2	12.9	16.7
$\mu^+ \mu^-$				
$G_e = 0$	$10^6$	$10^6$	$10^6$	
$G_e = G_m$	$10^6$	$10^6$	$10^6$	
$G_e = 3 \cdot G_m$	$10^6$	$10^6$	$10^6$	

Background:

$p \text{ (GeV/c)}$	1.7	3.3	5.9	7.9
$q^2 \text{ [(GeV/c)}^2]$	5.4	8.2	12.9	16.7
$\pi^+ \pi^-$		$10^8$	$10^8$	$2 \cdot 10^8$



# Comparison of electron and muon detection efficiencies



Plots by Gosia Sudol

Muon efficiency is **lower** than electron efficiency, due to **partial** implementation of the **muon** detector in the simulation.



## Test of muon identification with different cuts

### muon PID:

- 1 Very Loose (VL) > 20%
- 2 Loose (L) > 45%
- 3 Tight (T) > 70%
- 4 Very Tight (VT) > 85%
- 5 Likelihood (LH) > 90%
- 6 LH > 95%

### Kinematical fit:

- |                                                |                              |
|------------------------------------------------|------------------------------|
| 1 $CL(\mu^+\mu^-) > 10 \times CL(\pi^+\pi^-)$  | 1 $CL(\mu^+\mu^-) > 10^{-9}$ |
| 2 $CL(\mu^+\mu^-) > 50 \times CL(\pi^+\pi^-)$  | 2 $CL(\mu^+\mu^-) > 10^{-3}$ |
| 3 $CL(\mu^+\mu^-) > 100 \times CL(\pi^+\pi^-)$ | 3 $CL(\mu^+\mu^-) > 10^{-2}$ |
| 4 $CL(\mu^+\mu^-) > 150 \times CL(\pi^+\pi^-)$ | 4 $CL(\mu^+\mu^-) > 0.1$     |
| 5 $CL(\mu^+\mu^-) > 200 \times CL(\pi^+\pi^-)$ | 5 $CL(\mu^+\mu^-) > 0.4$     |
| 6 $CL(\mu^+\mu^-) > 300 \times CL(\pi^+\pi^-)$ | 6 $CL(\mu^+\mu^-) > 0.5$     |



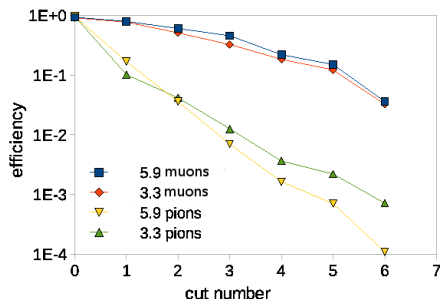


## Background suppression: Only PID cuts

$$3.3 \text{ GeV/c} - 8.2 \text{ (GeV/c)}^2$$

$$5.9 \text{ GeV/c} - 12.9 \text{ (GeV/c)}^2$$

Pid Cuts Efficiency  
Muon analysis



1 VL

2 L

3 T

4 VT

5 LH > 90%

6 LH > 95%

- The signal to noise ratio increases with LH level.

- The final cut has been selected to:

LH > 95%

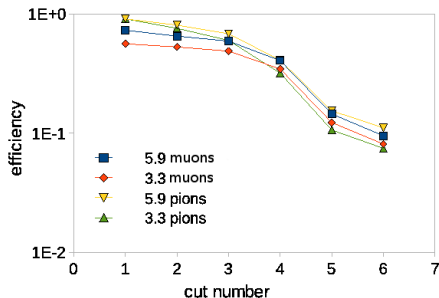


# Background suppression: Only kinematical fit cuts

$$3.3 \text{ GeV/c} - 8.2 \text{ (GeV/c)}^2$$

$$5.9 \text{ GeV/c} - 12.9 \text{ (GeV/c)}^2$$

Mu CL cuts  
Muon analysis



- ①  $CL(\mu^+\mu^-) > 10^{-9}$
- ②  $CL(\mu^+\mu^-) > 10^{-3}$
- ③  $CL(\mu^+\mu^-) > 10^{-2}$
- ④  $CL(\mu^+\mu^-) > 0.1$
- ⑤  $CL(\mu^+\mu^-) > 0.4$
- ⑥  $CL(\mu^+\mu^-) > 0.5$

- The  $\mu$  CL cut affects in the same way signal and background  
 $CL(\mu^+\mu^-) > 10^{-3}$

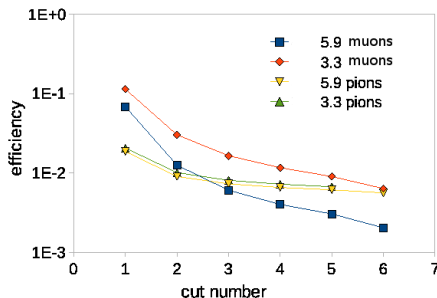


# Background suppression: Only kinematical fit cuts

$$3.3 \text{ GeV/c} - 8.2 \text{ (GeV/c)}^2$$

$$5.9 \text{ GeV/c} - 12.9 \text{ (GeV/c)}^2$$

## Mu Pi CL cuts muon analysis



- 1  $\text{CL}(\mu^+\mu^-) > 10 \times \text{CL}(\pi^+\pi^-)$
- 2  $\text{CL}(\mu^+\mu^-) > 50 \times \text{CL}(\pi^+\pi^-)$
- 3  $\text{CL}(\mu^+\mu^-) > 100 \times \text{CL}(\pi^+\pi^-)$
- 4  $\text{CL}(\mu^+\mu^-) > 150 \times \text{CL}(\pi^+\pi^-)$
- 5  $\text{CL}(\mu^+\mu^-) > 200 \times \text{CL}(\pi^+\pi^-)$
- 6  $\text{CL}(\mu^+\mu^-) > 300 \times \text{CL}(\pi^+\pi^-)$

- More restrictive cuts reduce the signal to noise ratio

- $\text{CL}(\mu^+\mu^-) > 10 \times \text{CL}(\pi^+\pi^-)$  and
- $\text{CL}(\mu^+\mu^-) > 50 \times \text{CL}(\pi^+\pi^-)$



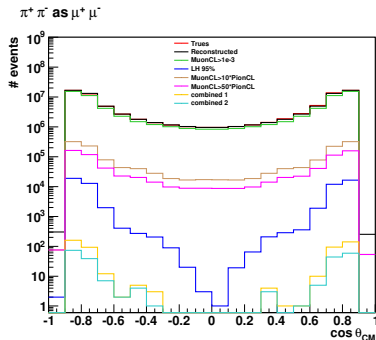
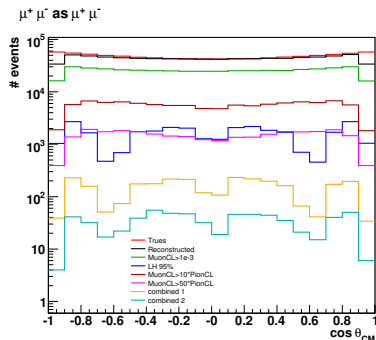
# Cuts effect on muons and pions angular distributions at 3.3 GeV/c - 8.2 (GeV/c)<sup>2</sup>

Signal: 1 000 000 events

Expected: 64 000 events

Background: 93 415 000 events

Expected:  $\approx 64 \cdot 10^9$  events



Combined 1: LH > 95%,  $CL(\mu) > 10^{-3}$  and  $CL(\mu) > 10 CL(\pi)$

Combined 2: LH > 95%,  $CL(\mu) > 10^{-3}$  and  $CL(\mu) > 50 CL(\pi)$



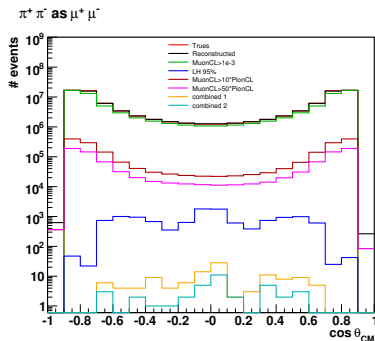
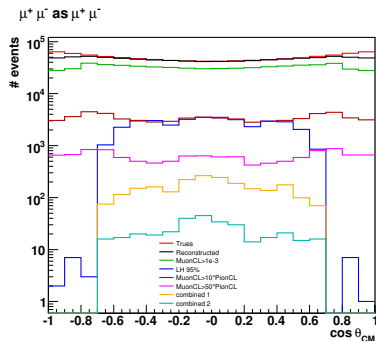
# Cuts effect on muons and pions angular distributions at 5.9 GeV/c - 12.9 (GeV/c)<sup>2</sup>

Signal: 1 000 000 events

Expected: 3 000 events

Background: 112 165 000 events

Expected:  $\approx 3 \cdot 10^9$  events



Combined 1: LH > 95%,  $CL(\mu) > 10^{-3}$  and  $CL(\mu) > 10 CL(\pi)$

Combined 2: LH > 95%,  $CL(\mu) > 10^{-3}$  and  $CL(\mu) > 50 CL(\pi)$



# Conclusions and Outlook

## ELECTRON ANALYSIS:

- Measurement of  $G_e/G_m$  is possible up to about  $14 \text{ (GeV/c)}^2$  by measurement of angular distribution.
- At higher energies is still possible to use the integrated cross section for Form Factors measurement.
- The error bars are reduced by a factor 10 in comparison with previous experiments.
- $\pi^+\pi^-$  background can be suppressed by a factor  $10^8$ .
- $\pi^0\pi^0$  background can be discriminated by kinematical constraints.

## MUON ANALYSIS:

- High background suppression implies drastic signal reduction in case of muons.
- Complete implementation of muon detectors in new software is needed.

PANDA detector at FAIR next to GSI seems to be of high utility for our measurements.